Marine and Petroleum Geology 27 (2010) 1107–1118

Contents lists available at ScienceDirect

Marine and Petroleum Geology

journal homepage: www.elsevier.com/locate/marpetgeo

Assessment of the oil source-rock potential of the Pedregoso Formation (Early Miocene) in the Falcón Basin of northwestern Venezuela

Jean Carlos Montero-Serrano [a,b,*], Manuel Martínez [a], Armelle Riboulleau [b], Nicolas Tribovillard [b], Gonzalo Márquez [c], José Vicente Gutiérrez-Martín [a]

[a] Instituto de Ciencias de la Tierra, Universidad Central de Venezuela. Apartado Postal 3895, Caracas 1010-A, Venezuela
[b] Université Lille 1, Laboratoire Géosystèmes, UMR 8157 CNRS, bâtiment SN5, 59655 Villeneuve d'Ascq cedex, France
[c] Departamento de Ingeniería Minera, Mecánica y Energética, Universidad de Huelva, Palos de Fra., 21819 Huelva, Spain

ARTICLE INFO

Article history:
Received 10 June 2009
Received in revised form
28 October 2009
Accepted 13 December 2009
Available online 29 December 2009

Keywords:
Geochemistry
Biomarkers
Redox conditions
Carbonate turbidites
Organic matter
Thermal maturity
Catagenesis
Venezuela
Falcón Basin

ABSTRACT

The early Miocene Pedregoso Formation is one of the numerous formations rich in organic matter within the stratigraphic record of the Urumaco Trough, in the central area of the Falcón Basin. Due to its lithological characteristics and stratigraphic position, this formation is of great interest regarding the basin's petroliferous systems. The evaluation of various inorganic and organic geochemical parameters indicates that the organic matter is primarily of marine origin, deposited in a marine carbonate environment typical of reefal systems, under oxic-to-dysoxic conditions. The low variability in the TOC concentrations and in the distributions of the biomarkers extracted from the samples suggests that the paleoenvironmental conditions and the organic-matter supply remained approximately constant throughout the sedimentation of this unit. The Pedregoso type-II organic matter (marine origin) and initial organic richness value (~1.8%) suggest that this unit has probably generated hydrocarbons within the Urumaco Trough. However, present-day thermal maturity parameters reveal that the Pedregoso organic matter is overmature (dry gas window), indicating that this unit is only capable to generate gas. In addition, the geothermal gradient, maturity parameters, and the maximum paleotemperature estimated in this study suggest that the Pedregoso Formation reached a maximum burial depth the ~6.5 km, consistent with the value obtained from data of stratigraphic thickness in the Urumaco Trough. This implies that the thermal anomaly that affected the basin during the Late Eocene–Early Miocene did not reach the central part of the basin, and therefore, the organic matter maturation in this unit is due to the sedimentary burial.

1. Introduction

The Falcón Basin in northwestern Venezuela (Fig. 1a), is an oil-containing marginal basin that, in spite of having scarce liquid hydrocarbon reservoirs, shows significant gas reserves and coal deposits. However, compared to the well-known Maracaibo, Barinas–Apure and Eastern Venezuela Basins (Fig. 1a), the petroliferous systems of the onshore Falcón Basin are poorly explored from the organic geochemistry point of view. In contrast, Oligocene–Miocene source rocks are well-known from the northern flank of the basin (offshore Falcón area); these rocks supplied hydrocarbons to a belt of small oilfields (Boesi and Goddard, 1991). In the stratigraphic column of the central region of the Falcón Basin, several units contain preserved organic matter (Boesi and Goddard, 1991; Del Ollo et al., 1994; Ghosh et al., 1997). One of them is the Pedregoso Formation (Early Miocene) deposited during a marine transgression (Macellari, 1995), and made of a rhythmic intercalations of dark marlstones with bioclastic limestones and sandstones that represent a turbiditic sedimentation (submarine fan) at the foot of the San Luis paleo-reef (Díaz de Gamero, 1977).

The lithological characteristics (calcareous rhythmic sequence; Fig. 1c) and the stratigraphical position (Early Miocene) confer to Pedregoso Formation a great interest in defining the petroliferous systems of the Falcón Basin (Ghosh et al., 1997). Nevertheless, the possible petroliferous systems of this basin have not been clearly established due to the structural complexity of the basin (Ostos et al.,

* Corresponding author. Université Lille 1, Laboratoire Géosystèmes, UMR 8157 CNRS, bâtiment SN5, 59655 Villeneuve d'Ascq cedex, France. Tel.: +33 320434395; fax: +33 320434910.
E-mail addresses: jeanmontero@yahoo.es (J.C. Montero-Serrano), manmarti@gmail.com (M. Martínez), armelle.riboulleau@univ-lille1.fr (A. Riboulleau), nicolas.tribovillard@univ-lille1.fr (N. Tribovillard), gmarmar@us.es (G. Márquez), jgutierr@ciens.ucv.ve (J.V. Gutiérrez-Martín).

0264-8172/$ – see front matter © 2009 Elsevier Ltd. All rights reserved.
doi:10.1016/j.marpetgeo.2009.12.007

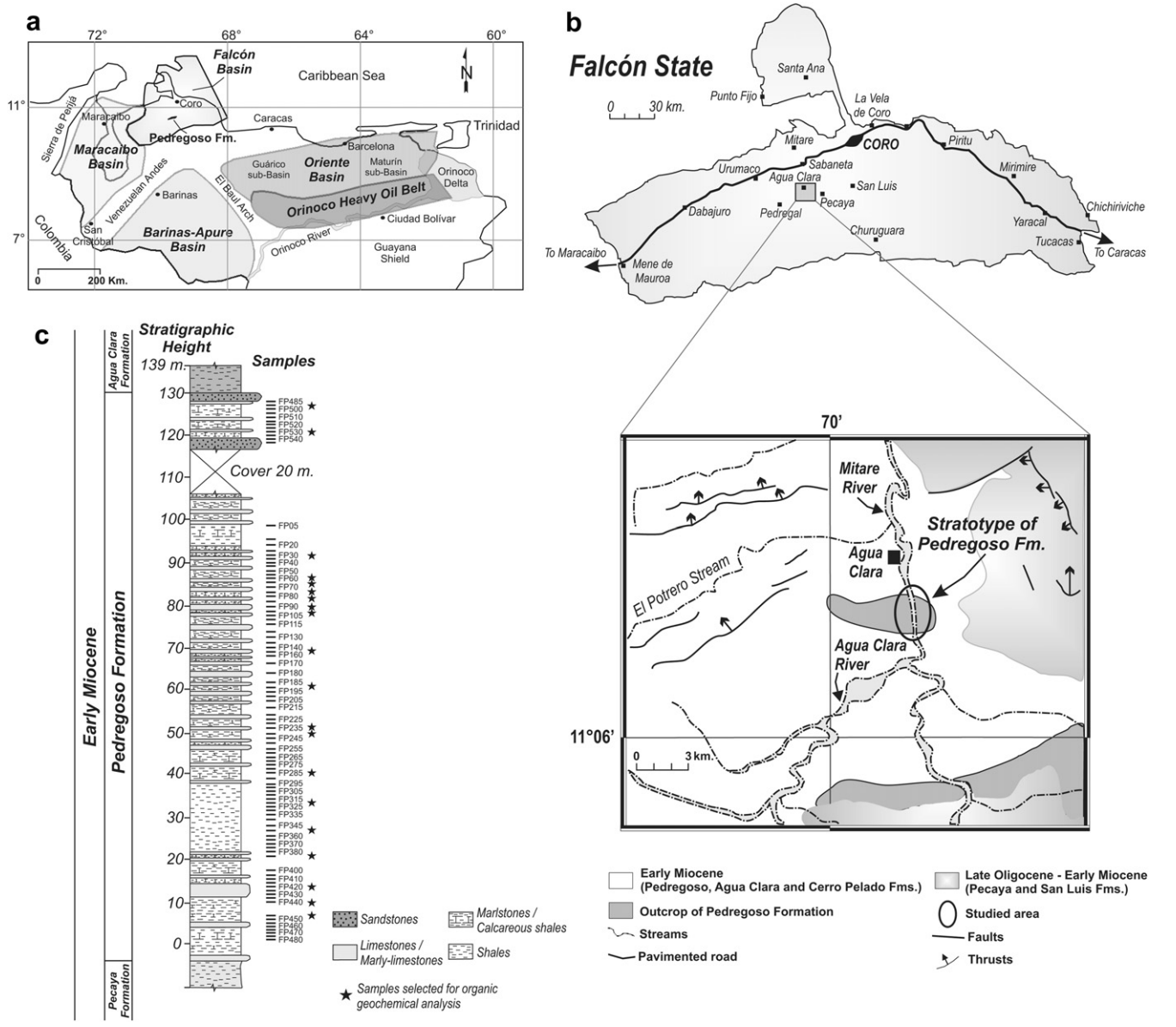

Fig. 1. a) Location of the petroliferous provinces of Venezuela (adapted from Ostos et al., 2005). The Pedregoso Formation (central part of the Falcón Basin) is marked; b) Simplified geological map of the Pedregoso Formation; c) Lithostratigraphic log of the Pedregoso Formation in the Mitare River (stratotype) showing location of samples.

2005) and the various possible source rocks (Boesi and Goddard, 1991). Until now, the overlying Agua Clara Formation had been considered one possible source of the crudes and oil seeps found in the Falcón Basin (Boesi and Goddard, 1991). However, we hypothesized that the organic matter preserved in the Pedregoso Formation may also be mature enough to be considered as a hydrocarbon source. Thus, since there are no previous organic geochemical studies on the organic matter preserved in the Pedregoso Formation, the aims of this study are to establish the paleo-oxygenation conditions controlling the accumulation and preservation of the organic matter of this unit and to determine the type of parental organic matter and the level of thermal maturity. This information can be very useful to future hydrocarbon exploration in the area.

2. Geological setting

The Falcón Basin has a peculiar position in northwestern South America, being located in the interaction zone between several major plates – Caribbean, Nazca and South America – and minor lithospheric blocks: Maracaibo, Bonaire and Western Colombia. Its sedimentary record, except for some unconformities of regional extent, was almost continuous from the late Eocene to the late Miocene (Audemard, 2001). Several studies have added significant information on the stratigraphy of the central region of the Falcón Basin (e.g., Audemard, 2001; Bezada et al., 2007). In the area of the Mitare River, the stratotype comprises the following formations, from bottom to top: El Paraíso, Pecaya, Pedregoso, Agua Clara, Cerro Pelado, Querales, Socorro and Urumaco (Fig. 2). All of these formations are Oligocene to Miocene and have been observed between the Urumaco and Mitare rivers. In general, the boundaries between these formations in the sedimentary sequence of the central region of the Falcón Basin are conformable and transitional. This region underwent strong subsidence during that period and is known in the literature as the Urumaco Trough (Díaz de Gamero, 1977).

During the Late Eocene, the Falcón Basin underwent erosion. A new transgressive cycle began with the deposition of the sediments

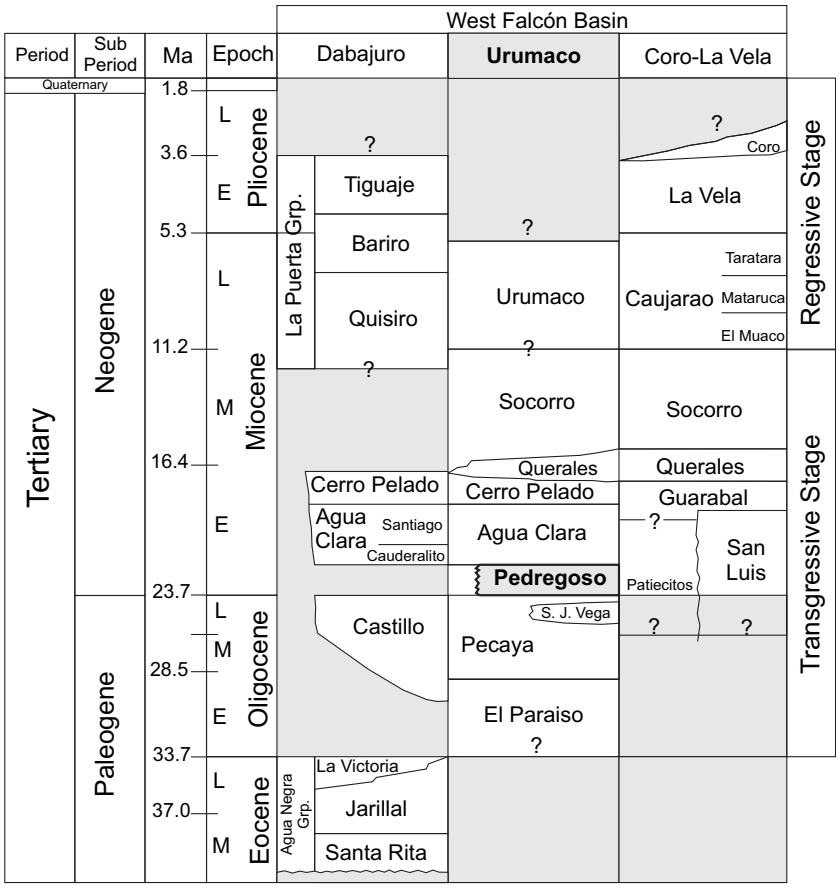

Fig. 2. Stratigraphic correlation of map units for the subsurface and surrounding areas of the west Falcón Basin. Modified from Díaz de Gamero (1997) according to the Código Estratigráfico de las Cuencas Petroleras de Venezuela (PDVSA, 2009). Inset shows the locations where strata are present at surface.

of the El Paraíso Formation (Early Oligocene), comprising sandy facies interstratified with shales and coals (González de Juana et al., 1980). Subsequently, according to Díaz de Gamero (1977), basin depth (~1000 m) increased, as evidenced by the first signs of open-sea influence, in relation to a strong subsidence. A thick sequence of silty black shales, part of the Pecaya Formation (Middle Oligocene–Early Miocene) deposited in this setting. On top of this formation, the Pedregoso Formation, deposited during the Early Miocene, lies conformably and transitionally (Fig. 2).

The tectonic subsidence in the basin culminated at the Oligocene–Miocene boundary with the last basaltic intrusions and sedimentary colmatation (Audemard, 2001); then, the sedimentary sequences became progressively less-marine. During the Early Miocene, there was conformable deposition over the Pedregoso Formation consisting of slightly calcareous black shales with scarce intercalations of siltstones and sandstones, known as the Agua Clara Formation (Fig. 2). Next, the sandstones, shales, and coals comprising the Cerro Pelado Formation are overlying (Díaz de Gamero, 1989). This formation represents a transition from the marine environment of the underlying Agua Clara Formation to the very near-shore to coastal plain environment that prevailed when the overlying Querales Formation was deposited (Early Miocene-Middle Miocene). The Querales Formation is dominated by black shales with intercalations of fine-grained sandstones and occasional marls and limestones. Immediately above is the sediments of the Socorro Formation (Middle Miocene), consisting of alternating sequences of sandstones, siltstones, shales, and limestones. At the end of the Miocene began the Andean uplift, during which the basin was intensely folded and tectonically inverted by NW-SE compression. As a consequence, the sea began to retreat northeastward (regression stage) and coastal–continental facies were deposited, as represented by the Urumaco Formation (Late Miocene) (Díaz de Gamero, 1989) (Fig. 2).

The lithology of the Pedregoso Formation (Fig. 1c) consists of dark marlstones (hard and silty) with rhythmically interbedded bioclastic limestones and rare sandstones. The limestone and sandstone layers are <1 m thick. The limestones, generally allodapic and dark gray, dominates on the half of the unit (Fig. 1c). The proportion of detrital quartz grains, chert, and rock fragments increases topward in the type section. The siltstones are dark gray, calcareous, and commonly have small ripples in the upper part. The sandstones located in the upper part of the formation are fine-grained and slightly calcareous. Based on field relationships, sedimentology, and fossil content, Díaz de Gamero (1977) interpreted the Pedregoso Formation as a wedge-shaped sheet of carbonate turbidites deposited as a submarine fan in the deep-water (<1000 m) facies of the Pecaya Formation located at the base of the reef preserved in the San Luis Formation.

3. Materials and methods

We collected 98 rock samples along the about 130 m (~1 sample/meter) of the stratigraphic column of the type section of the Pedregoso Formation, cropping out in the Mitare River (Fig. 1c). An aliquot (about 500 g) of each sample was crushed and pulverized using a Shatterbox with a wolframium carbide grinding container. Later, each sample was sieved through 100 mesh size in order to homogenize the degree of pulverization.

Total carbon (C) was determined by combustion at 950 °C using a LECO C-144 instrument. Total inorganic carbon (TIC) content was determined as a calcium carbonate ($CaCO_3$) percentage through Bernard's calcimeter method (Hesse, 1971) using a CORAL-1 apparatus. Total organic carbon (TOC) is calculated as the difference between the C values and the TIC values. Since the Pedregoso Formation samples have high contents of the sulfate-type evaporites (Noya, 2001), the reduced sulfur (S_{red}) concentration was determined from the residue of the digestion with 1 M HCl for 8 h at room temperature, since most of the sulfate is eliminated in an acid medium. The resultant residue was filtered, washed with abundant distilled water, dried for 48 h at 40 °C, and subsequently weighted. The reduced sulfur determination was made with a LECO SC-432 instrument at 1350 °C for 6 min. In addition, the residue of the 1 M HCl digestion was also used to determine the TOC concentration in the carbonate-free fraction using a LECO C-144 instrument.

The degree of pyritization (DOP), defined as the ratio of pyritic iron to the reactive iron fraction (Berner, 1984; Raiswell et al., 1987), was systematically determined for 44 samples (2.5 g each) throughout the stratigraphic column. Pyritic and reactive iron concentrations were measured using replicate samples by leaching with 10 ml of concentrated HNO_3 and by the 1 N HCl procedure (20 ml, 16 h), respectively (Huerta-Díaz and Morse, 1990). Fe concentrations were determined by flame atomic absorption spectrometry by using a 703 Perkin-Elmer spectrometer. Accuracy of the iron content analysis (±2%) was tested with AN-G (anorthosite) geostandard. The limit of determination (LOD) was 0.0001 wt./wt. The Fe concentrations were measured at two wavelengths, 248 nm and 372 nm.

The T_{max} index (°C), which is an indicator of thermal maturity of the organic matter (OM), was determined in nine samples on 100 mg of ground bulk-rock sample with a Delsi Oil Show Analyzer (see Espitalié et al., 1986 for procedural details) at the Université Paris 6, France.

Elemental and biomarker analyses were performed on 20 samples distributed throughout the stratigraphic column (Fig. 1c), with total organic carbon contents of 0.18–1.25%. Quantification of carbon (C), hydrogen (H), oxygen (O), nitrogen (N), and sulfur (S) contents in the kerogen concentrate were carried out using a Thermo Flash EA1112 elemental analyzer. Previously, the kerogen concentrate was isolated from the pulverized rock sample (approximately 10 g) through HCl–HF acid digestion (Vandenbroucke and Largeau, 2007). Precision was better than 2% for C, and 4% for H, O, N, and S based on international standards and replicate samples. Approximately 185 g of ground samples were extracted for 72 h with a Soxhlet apparatus using recently distilled (over calcium chloride) dichloromethane as solvent. During bitumen extraction, elemental sulfur was removed by adding "copper turnings previously washed in acid and solvent". Later, the solvent was removed using a rotary evaporator and the bitumen thus obtained was fractionated by microcolumn chromatography using a Pasteur pipette. The absorbent used was activated (200 °C for 48 h) neutral alumina with activity No. 1. Before activation, the alumina was rinsed with methanol. The saturates were eluted with *n*-hexane and the aromatics with toluene. Fractions were recovered by fractional distillation of the solvent. Later, the saturated hydrocarbons were rechromatographed to eliminate possible contamination with aromatic hydrocarbons. Aliquots of saturated and aromatic hydrocarbons were subsequently analyzed using gas chromatography-mass spectrometry (GC–MS) with an Agilent Technologies (AT) 6890N gas chromatograph (on column injection; AT-HP-5MS capillary column, 30 m × 0.25 mm internal diameter; film thickness 0.25 μm; Helium was used as carrier gas) coupled to an AT 5975 mass spectrometer (full-scan mode; 70 eV). Oven temperature was programmed from 80 to 270 °C at 30 °C/min, then to 300 °C at 10 °C/min. Biomarkers were identified by comparison of mass spectra, retention times and mass chromatography of diagnostic ions available in the literature. The relative contents of particular compounds were calculated from peak height.

4. Results and interpretations

4.1. Bulk geochemical data

The stratigraphical distributions of the values of the TOC, $CaCO_3$, S, and the DOP for the Pedregoso Formation are presented in Fig. 3. The calcium carbonate weight percent varies between 0.1 and 87.6% and samples with values between 2 and 29% $CaCO_3$ are dominant. Calcareous shale is the most common of rock type and occurs throughout the section, but is more abundant in the middle stratigraphic unit. The TOC ranges between 0.11 and 1.25%. Higher TOC values are present in the calcareous shale intervals (average 0.85%). The TOC values decrease from 0.85% for calcareous shales to 0.45% for marls down to 0.25% for limestones and marly limestones. Reduced sulfur (S_{red}) values range from 0.01 to 0.88% (average 0.17%).

A negative correlation is observed between the $CaCO_3$ content and the TOC. The dilution of the TOC concentration by carbonate was corrected by calculating the TOC content in the carbonate-free fraction (TOC_{CFF}). Results indicate that the TOC_{CFF} concentration fluctuates around 1% throughout the unit, regardless of the lithology (Fig. 3). It indicates that the supply and preservation of OM was approximately constant during the sedimentation of the Pedregoso Formation.

On the other hand, it is important to have a measure of the effective organic carbon content, i.e., the portion of the TOC which is converted to petroleum during burial to great depths and temperatures (Tissot and Welte, 1984; Hunt, 1995). Thus, using a typical approach, we have also corrected TOC_{CFF} values for maturity effects (see below), the initial organic richness (TOC°) can be approximately calculated as:

$$TOC^{\circ} \times [HI^{\circ} - F \times (HI^{\circ} - HI)] = TOC_{CFF} \times HI^{\circ}$$

In this formula, F, HI, and HI° are theoretical maximum percent of TOC convertible to the carbon of hydrocarbons (~48%, type-II kerogen), measured present-day and original Hydrogen Index values ~550 and ~30 mg of HC per gram of TOC, respectively (Hunt, 1995). Thus the initial organic richness value (~1.8%) suggests that the Pedregoso Formation can be considered as a potential source rock within the Urumaco Trough ($TOC^{\circ} > 1\%$; Hunt, 1995).

4.2. Paleo-oxygenation conditions

A ternary TOC–S–Fe diagram was drawn using the TOC and S concentrations from this study and the total Fe concentrations reported by Rojas (2001) in order to determine the paleo-oxygenation conditions predominating during the deposition of the Pedregoso Formation sediments (Fig. 4). The TOC–S–Fe relationship is commonly used to distinguish marine from continental environments as well as to evaluate paleo-oxygenation conditions in the sedimentary environment (Dean and Arthur, 1989; Rimmer et al., 2004).

Fig. 3 shows that some of the samples lie near the line representing the S/C ratio of 0.4 ($DOP_{stoichiometric} < 0.42$), which indicates that deposition occurred in a marine environment under oxic conditions. The rest of the samples plot between the lines representing S/Fe ratios of 0.30–0.42 ($DOP_{stoichiometric}$ values from 0.56 to

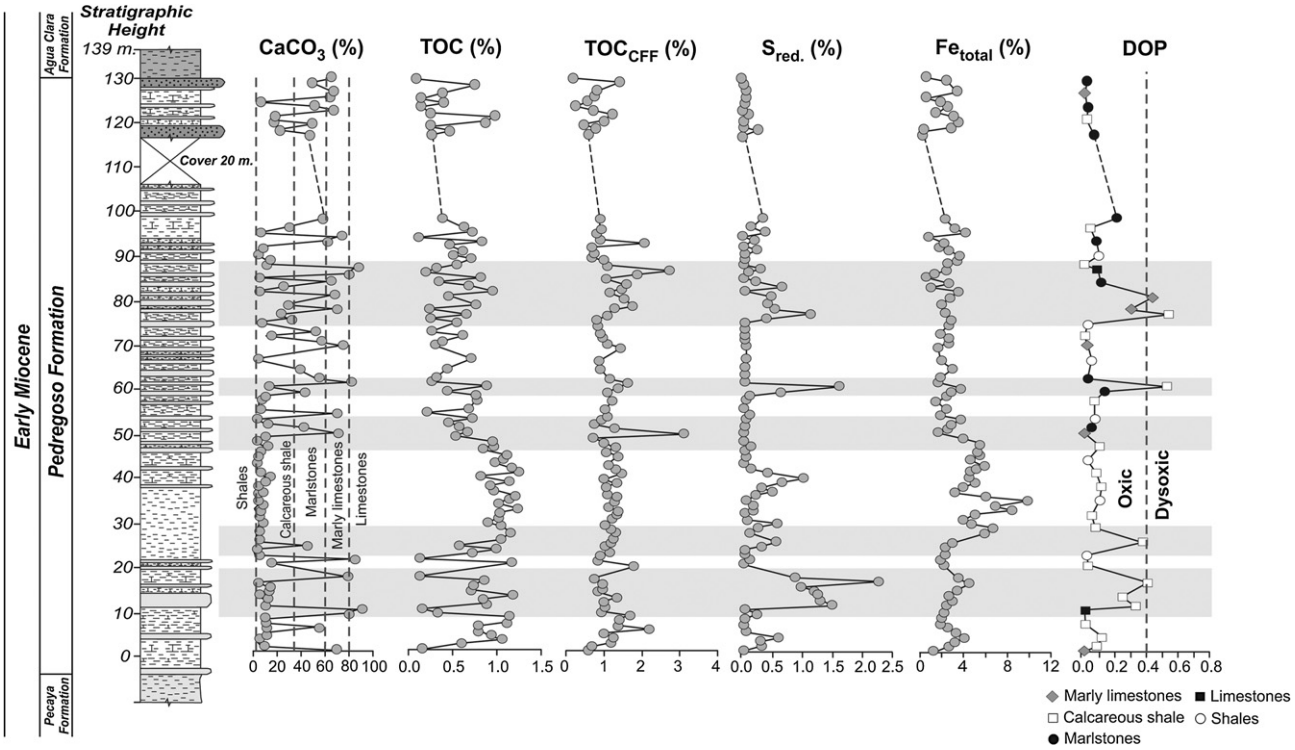

Fig. 3. Stratigraphic distribution of the concentrations (% wt.) of $CaCO_3$, TOC, TOC_{CFF}, $S_{red.}$, total Fe (Rojas, 2001), and values of the degree of pyritization (DOP) from the Pedregoso Formation.

0.78), indicating dysoxic conditions and a poorly stratified water column (Berner, 1984). Experimental DOP data also corroborate variations in the degree of oxygenation during deposition of the sediments of the Pedregoso Formation. $DOP_{exp.}$ values vary from 0.01 to 0.55 (average 0.15), pointing to the predominance of oxic ($DOP_{exp.} < 0.4$) to dysoxic ($DOP_{exp.} > 0.4$) conditions in the depositional environment (Fig. 3).

4.3. Kerogen elemental composition

Table 1 gives the abundance in soluble OM (bitumen), the relative proportions of the fractions analyzed (saturates and aromatics), and the atomic ratios (H/C, O/C, S/C, N/C) of the kerogen concentrate isolated from the rock samples.

In the kerogen concentrate, the sum of C, H, N, O and S contents ranges between 51 and 74%. This incomplete mass balance largely suggests that the isolated kerogen contains some residual minerals. This fact can entail to an overestimation of H and O contents (e.g., Vandenbroucke and Largeau, 2007). Considering this aspect, only an estimation of the bulk composition of the organic phase can be reported in this study (Table 1). Concurrently, the H/C ratio ranges from 0.25 to 0.81 (average 0.53) and the O/C ratio varies from 0.11 to 0.94 (average 0.40). These ratios suggest that the OM is oxidized and/or highly mature (in the late stage of catagenesis). At this stage of maturity, the most abundant functional groups in OM are the aromatics, and the oil that could have been generated previously was expelled and the remaining OM is only capable to generate gas. Tissot et al. (1980) term this type of kerogen as type IV ($H/C < 0.6$; residual OM). The S/C ratio ranges from 0.01 to 1.21 (average 0.24),

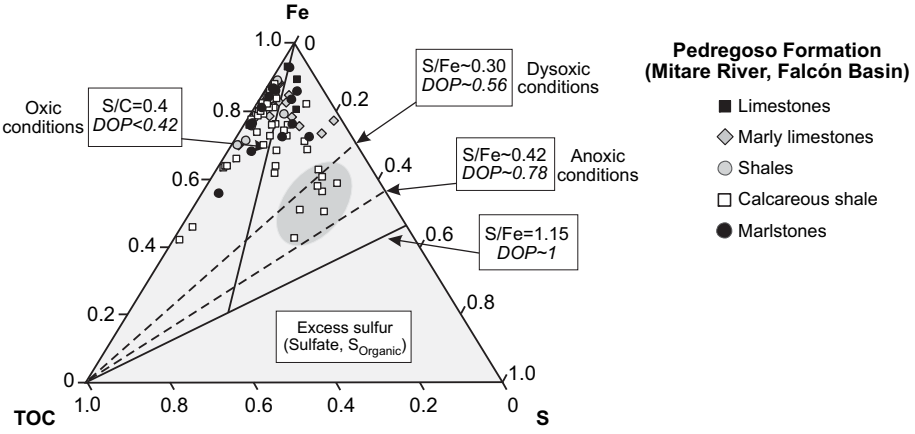

Fig. 4. COT–S–Fe ternary diagram corresponding to the Pedregoso Formation.

Table 1
Stratigraphic height, lithology, atomic ratios of kerogen concentrates and extracted bitumen data for Pedregoso samples.

Sample	Height	Lithology	H/C	O/C	S/C	N/C	Bitumen	Saturates	Aromatics
FP-490	128	Marlstone	0.73	0.33	0.05	0.032	75	20	19
FP-530	122	Limy shale	0.47	0.17	0.06	0.020	41	13	12
FP-30	92	Marlstone	0.49	0.18	0.09	0.021	50	28	14
FP-60	86	Shale	0.52	0.34	0.39	0.015	57	29	15
FP-65	85	Marly lime	0.50	0.27	0.17	0.022	55	28	13
FP-75	83	Marlstone	0.62	0.30	0.26	0.019	65	32	8
FP-80	82	Limy shale	0.81	0.74	0.35	0.024	52	27	17
FP-90	80	Marly lime	0.62	0.94	1.21	0.023	218	134	35
FP-100	78	Limy shale	0.55	0.55	0.18	0.019	42	21	20
FP-145	69	Marly lime	0.53	0.20	0.07	0.020	52	19	17
FP-190	60	Limy shale	0.56	0.78	0.65	0.017	63	31	29
FP-235	51	Marlstone	0.68	0.72	0.01	0.018	41	9	10
FP-240	50	Marly lime	0.51	0.13	0.02	0.015	25	2	6
FP-285	41	Limy shale	0.69	0.89	0.11	0.021	133	7	67
FP-320	34	Limy shale	0.41	0.11	0.04	0.016	56	19	20
FP-350	28	Limy shale	0.46	0.16	0.03	0.018	79	31	19
FP-385	21	Limy shale	0.25	0.46	0.03	0.016	51	18	16
FP-420	14	Limy shale	0.33	0.35	0.47	0.015	50	17	15
FP-440	10	Marly lime	0.48	0.12	0.26	0.009	59	30	14
FP-455	7	Marlstone	0.45	0.23	0.17	0.007	32	15	8

Note: Bitumen, aromatics and saturates contents are expressed in mg/kg; stratigraphic heights in meters.

these anomalously high values indicate the presence of pyrite in the isolated OM, consistent with the high DOP values in these intervals (Fig. 3). The N/C atomic ratio in the Pedregoso Formation ranges from 0.007 to 0.032 (average 0.018). According to Hetényi et al. (2004) and Vandenbroucke and Largeau (2007), these low values also can suggest that the preserved OM underwent selective degradation during early diagenesis and thermal alteration, causing a loss of heteroatoms from the kerogen.

4.4. Origin of the organic matter

The *m/z* 99 fragmentograms for the saturated fraction show similar *n*-alkane distributions for all the samples, with unimodal distribution in the *n*-C_{14} or *n*-C_{35} interval, a maximum at *n*-C_{16} or *n*-C_{18} (CCL values >0.6, relationship between short- and long-chain *n*-alkanes; Fig. 5, Table 2), and even-carbon-numbered predominance in the range *n*-C_{14} to *n*-C_{24}. In general, such a distribution with predominance of short-chain (<*n*-C_{20}) compounds, is characteristic of prevalently marine OM (e.g., Gelpi et al., 1970; Blumer et al., 1971). Toward the top of the unit, sample FP-490 shows a bimodal *n*-alkane distribution (CCL values 0.5; Table 2), with a second maximum in *n*-C_{29} (Fig. 5), indicating a pulse of terrigenous OM (e.g., Peters et al., 2005).

The distribution of terpanes (*m/z* 191) and regular steranes (*m/z* 217) is similar for all the samples (Fig. 6). The *m/z* 191 fragmentograms show that the tricyclic terpanes range from $C_{19\text{-}3}$ to $C_{29\text{-}3}$, with a typical maximum at $C_{23\text{-}3}$. The presence of tricyclic terpanes and the high $C_{23\text{-}3}/C_{24\text{-}4}$ ratios in all the samples (Table 2) suggest a high contribution of marine OM (Ourisson et al., 1982). However, it must be recalled that the concentration of tricyclic terpanes increases with thermal maturation (Peters et al., 2005).

The *m/z* 191 fragmentograms (Fig. 6) show the dominance of the C_{27}–C_{35} series of hopanes and homohopanes (pseudo-homologues: C_{31}–C_{35}), which indicates bacterial contributions to OM in the Pedregoso Formation. Both series possess the 17α(H),21β(H) configuration and extended C_{31} to C_{35} members occur as doublets of 22S and 22R isomers (Fig. 6). The hopanoids (e.g., hopanes, hopenes) are derived mainly from hopane polyols (e.g., bacteriohopanetetrol) occurring in the lipid membranes of many procaryotic organisms (Ourisson and Albrecht, 1992; Ourisson and Rohmer, 1992).

In the *m/z* 191 fragmentograms (Fig. 6) of all the samples we tentatively identified 18α(H)-oleanane, a terrestrial biomarker (e.g., Ekweozor and Udo, 1987; Alberdi and López, 2000). However, its low abundance relative to the C_{30} hopane in most of the samples (see Table 2) is evidence of a low supply of terrestrial OM during Pedregoso Formation sedimentation. Alternatively, this compound may correspond to lupane or some minor C_{30} compounds of non-terrigenous origin having lupane-like mass spectra (Nytoft et al., 2002).

The distribution of the regular steranes in the m/*z* 217 fragmentograms (Fig. 6) shows a high proportion of C_{27} sterane compared to C_{28} and C_{29}. The relative abundance of regular steranes, C_{27}, C_{28}, and C_{29}, is often used to determine the dominant source of OM since C_{27} sterols derive mainly from zooplankton, C_{28} sterols from phytoplankton, and C_{29} sterols are abundant in land plants (Huang and Meinschein, 1979). Although more recent research has demonstrated that C_{29} sterols are also present in numerous microalgae such as diatoms and freshwater eustigmatophytes (Volkman et al., 1998), the sterane ternary plot is still useful in reflecting the source of sedimentary OM and petroleum. The distribution patterns of regular steranes of most samples plot in the marine part of the ternary diagram (Fig. 7), confirming the predominance of sterol derived from marine organisms (algae) compared to those from land organisms.

4.5. Paleoenvironmental conditions

One of the most commonly used parameter for the study of paleo-oxygenation conditions in sedimentary sequences is the pristane/phytane (Pr/Ph) ratio (Peters et al., 2005). In this particular stratigraphic sequence, the Pr/Ph ratio, determined in the *m/z* 183 fragmentograms (Fig. 5), generally ranges from 1.06 to 1.77 (average 1.36) (Table 2), indicating that the OM was deposited under oxic-to-dysoxic conditions. A possible impact of the thermal maturity must be considered when using the Pr/Ph ratio (e.g., Dzou et al., 1995; Koopmans et al., 1999), however this interpretation is in agreement with the other indicators of paleo-oxygenation conditions (C–S–Fe and DOP) used in this study.

The relationship between dibenzothiophene/phenantrene (DBT/P) and pristane/phytane (Pr/Ph) is used as a paleodepositional-environment indicator of sedimentary rocks. Hughes et al. (1995) propose that the DBT/P (*m/z* 178 + 184) ratio evaluates the

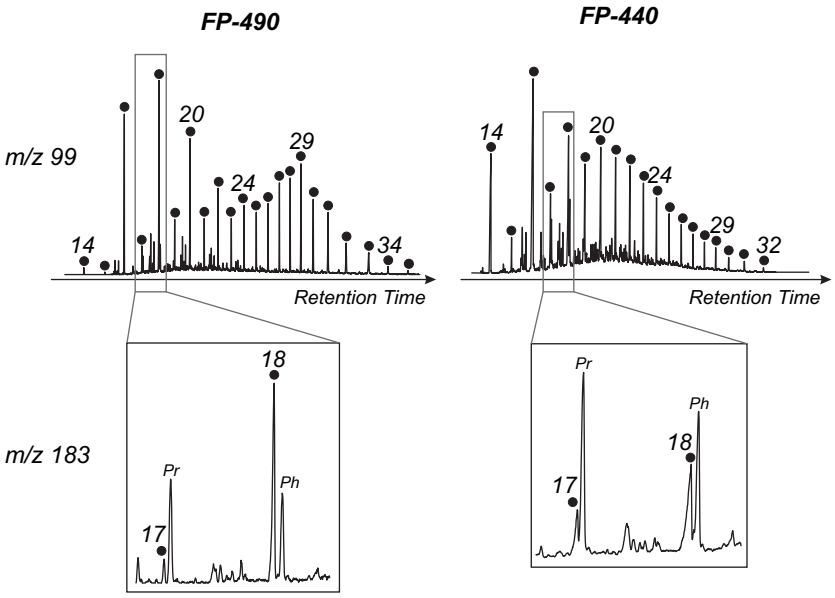

Fig. 5. *m*/*z* 99 and *m*/*z* 183 ion fragmentograms showing *n*-alkane and acyclic isoprenoids (Pr: Pristane; Ph: Phytane) distributions for two representative samples (FP-440 and FP-490, base and top of the Perdregoso Formation, respectively).

availability of reduced sulfur that becomes incorporated in the OM and that, in contrast, the Pr/Ph (*m*/*z* 183) ratio indicates the reducing conditions of the depositional environment. In general, the samples studied herein lie within the marine carbonate field poor in OM and marine shale (Fig. 8), confirming the marine paleoenvironmental interpretation.

4.6. Thermal maturity

Various indicators based on biomarker distribution have been determined to evaluate the thermal maturity level of the OM in the Pedregoso Formation. The values for the CPI (carbon preference index; Bray and Evans, 1961) are about 1.1 for most of the samples (Table 2), which shows the lack of a strong even/odd-carbon-number predominance of *n*-alkanes. This lack of predominance may be caused by the high maturation level of the OM.

The relative abundance of 22S and 22R homohopanes and 20S and 20R steranes (average values of 0.59 and 0.48 respectively; Table 2), indicates that the racemization has reached the equilibrium point for both series. These results suggest that the thermal maturity of the OM has at least reached the gas-generation stage (late catagenesis, %Ro $>$ 1.35; Hunt, 1995; Peters et al., 2005).

Consequently, several parameters based on the distribution of aromatic biomarkers (e.g., Radke and Welte, 1983; Alexander et al., 1986) have been determined to evaluate more precisely the thermal maturation of the OM in the Pedregoso Formation. The indices involving aromatic hydrocarbons and aromatic sulfur compounds can reflect a wide range of maturity, from early

Table 2
Molecular parameters for saturate fractions in extracted bitumen samples from Pedregoso Formation.

Sample	CPI	Pr/Ph	CCL	$C_{23\text{-}3}/C_{24\text{-}4}$	Oleanane/C_{30} hopane (%)	$C_{31}\alpha\beta$ 22S/(22S + 22R)	$C_{29}\alpha\alpha\alpha$ 20S/(20S + 20R)	C_{27}/C_{29} sterane
FP-490	1.12	1.22	0.46	4.28	9.98	0.58	0.47	1.55
FP-530	1.20	8.04	0.81	4.59	9.02	0.56	0.48	1.54
FP-30	0.99	1.06	0.66	3.32	8.72	0.57	0.50	1.24
FP-60	1.20	1.74	0.66	6.05	8.88	0.63	0.46	1.63
FP-65	1.19	1.52	0.64	2.29	8.24	0.60	0.49	1.51
FP-75	1.02	1.64	0.89	–	9.36	0.52	–	–
FP-80	1.09	1.08	0.74	4.73	8.38	0.59	0.50	1.40
FP-90	1.09	1.21	0.71	4.54	14.29	0.55	0.50	1.18
FP-100	1.18	1.77	0.89	4.15	8.68	0.56	0.70	1.11
FP-145	1.20	1.30	0.72	6.17	8.79	0.59	0.36	1.94
FP-190	1.26	1.42	0.90	2.65	9.13	0.56	0.55	1.34
FP-235	1.21	1.20	0.69	4.53	7.56	0.58	0.37	2.54
FP-240	0.91	1.36	0.81	–	15.36	0.60	–	–
FP-285	1.14	1.34	0.84	–	–	–	–	–
FP-320	1.07	1.36	0.79	3.50	8.70	0.61	0.46	1.77
FP-350	1.12	8.69	0.90	4.38	8.84	0.57	0.55	2.30
FP-385	1.53	1.33	0.70	5.17	7.94	0.58	0.49	1.66
FP-420	1.17	2.67	0.64	3.12	7.94	0.58	0.49	1.52
FP-440	1.07	1.29	0.59	4.83	9.32	0.58	0.46	1.43
FP-455	1.18	1.36	0.66	6.65	15.50	0.60	0.52	2.51

$CPI = 2\cdot n\text{-}C_{22+25+27+29}/(n\text{-}C_{22} + n\text{-}C_{30} + 2\cdot n\text{-}C_{24+26+28})$ (Bray and Evans, 1961).
$CCL = n\text{-}C_{12\text{-}20}/n\text{-}C_{12\text{-}29}$; $C_{23\text{-}3}/C_{24\text{-}4} = C_{23}$-tricyclic terpane/$C_{24}$-tetracyclic terpane.
$C_{31}\alpha\beta$ 22S/(22S + 22R) = 17α,21β(H)-29-homohopane 22S and 22R.
$C_{29}\alpha\alpha\alpha$ 20S/(20S + 20R) = 5α,14α,17α(H)-stigmastane 20S and 20R.

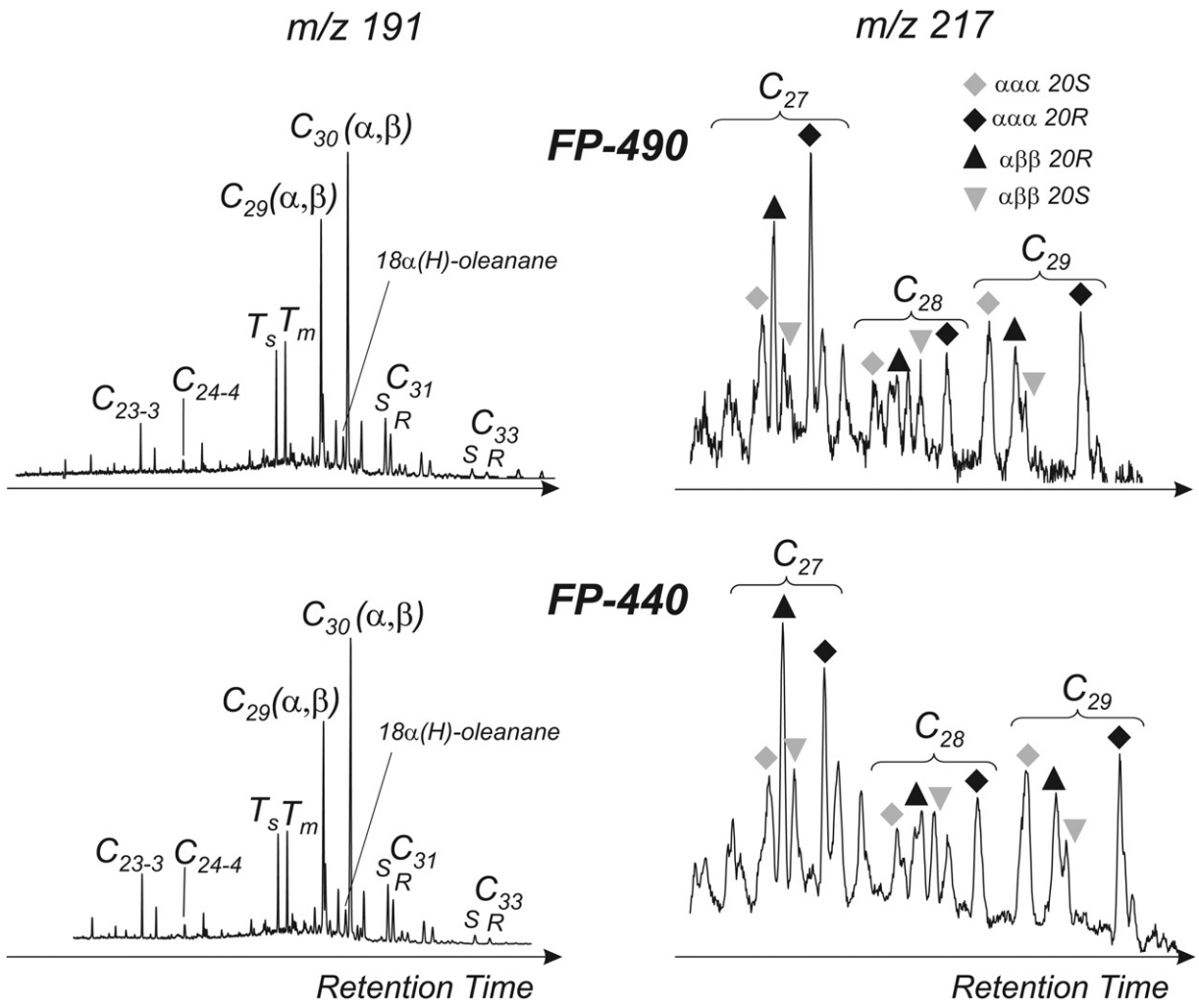

Fig. 6. *m/z* 191 and *m/z* 217 ion fragmentograms showing terpanes and regular steranes distributions for two characteristic samples (FP-440 and FP-490). $C_{23\text{-}3}$: 23 tricyclic terpane; $C_{24\text{-}4}$: 24 tetracyclic terpane; Ts: 18α(H)-22,29,30 trisnorneohopane; Tm: 17α(H)-22,29,30 trisnorhopane; C_{29}(α,β): C_{29}-17α,21β(H)-30-norhopane; C_{30}(α,β): C_{30}-17α,21β(H)-hopane; C_{31}: C_{31}-17α,21β(H)-29-homohopane 22S and 22R; C_{33}: C_{33}-17α,21β(H)-29-trishomohopane 22S and 22R.

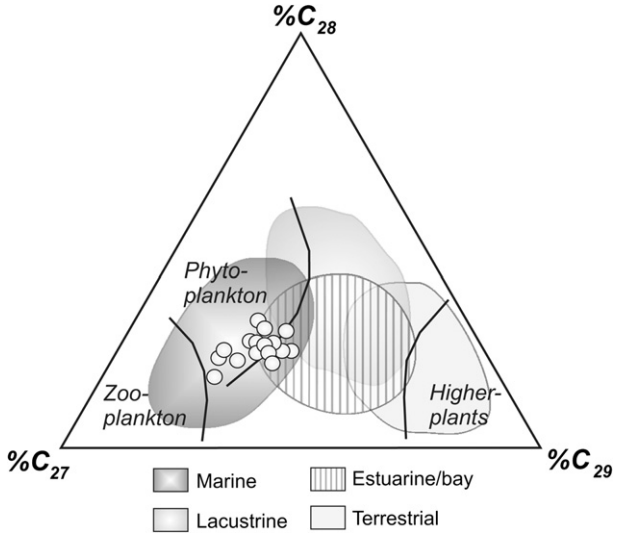

Fig. 7. Ternary plot showing contribution of C_{27}, C_{28} and C_{29} ααα and αββ regular steranes. Paleoenvironmental and source interpretation according to Huang and Meinschein (1979).

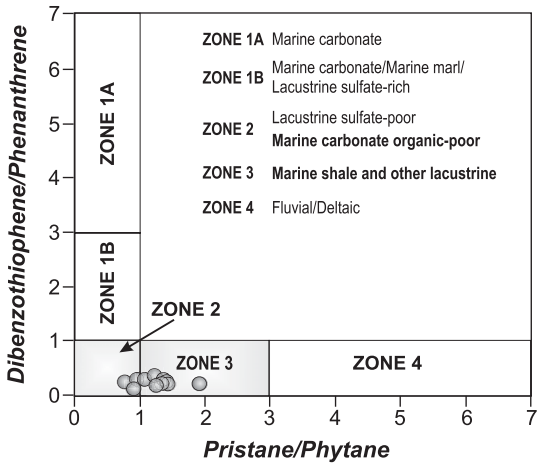

Fig. 8. Cross-plot of the dibenzothiophene/phenanthrene (DBT/P) vs. pristane/phytane (Pr/Ph) ratios. Paleoenvironmental and source interpretation according to Hughes et al. (1995).

Table 3
Molecular parameters for aromatic fractions in extracted bitumen samples and T_{max} values from Pedregoso Formation.

Sample	TMNr	TeMNr	MPI-1	MPR	%Rc$_1$	MDR	%Rc$_2$	DBT/P	T_{max} (°C)
FP-490	0.53	0.53	0.75	1.86	–	3.40	1.23	0.25	–
FP-530	0.66	0.74	0.09	3.39	2.24	5.75	1.36	0.06	–
FP-30	0.57	0.55	0.33	2.83	2.10	5.87	1.37	0.22	483
FP-60	0.45	0.68	0.62	2.55	–	4.18	1.28	0.25	490
FP-65	0.60	0.71	0.42	2.70	2.05	4.78	1.32	0.26	491
FP-75	0.60	0.68	0.40	3.36	2.06	6.94	1.41	0.24	–
FP-80	0.41	0.64	0.38	3.68	2.07	7.06	1.42	0.21	–
FP-90	0.56	0.72	0.64	1.83	–	3.46	1.23	0.29	490
FP-100	0.65	0.69	0.43	3.94	2.04	8.10	1.45	0.21	478
FP-145	0.65	0.73	0.37	2.26	–	4.34	1.29	0.27	480
FP-190	0.56	0.58	0.27	3.35	2.14	8.47	1.47	0.21	482
FP-235	0.43	0.62	0.31	2.12	–	3.82	1.26	0.15	490
FP-240	–	–	0.55	2.73	1.97	–	–	0.14	–
FP-285	0.65	0.73	0.10	3.45	2.24	6.36	1.39	0.06	–
FP-320	0.67	0.74	0.19	4.21	2.19	7.90	1.45	0.20	–
FP-350	0.60	0.64	0.41	2.79	2.05	6.03	1.38	0.21	–
FP-385	0.65	0.75	0.53	1.86	–	3.99	1.27	0.31	483
FP-420	0.62	0.66	0.23	5.00	2.16	13.85	1.60	0.20	–
FP-440	0.62	0.68	0.37	2.73	2.08	4.75	1.31	0.30	–
FP-455	0.45	0.67	0.55	2.43	–	3.68	1.25	0.23	–

TMNr = 1,3,7-TMN/[1,3,7-TMN + 1,2,5-TMN] (van Aarssen et al., 1999).
TeMNr = 1,3,6,7-TeMN/[(1,3,6,7 + 1,2,5,6 + 1,2,3,5)-TeMN] (van Aarssen et al., 1999).
MPI-1 = 1.5·[2-MP+3-MP]/[P+1-MP+9-MP] (Radke and Welte, 1983).
MPR = 2-MP/1-MP (Radke and Welte, 1983).
%Rc$_1$ = −0.60· MPI-1 + 2.30 [MPR > 2.65] (Radke and Welte, 1983).
MDR = 4-MDBT/1-MDBT (Radke et al., 1986)
%Rc$_2$ = 0.2633·Ln(MDR)+0.9034 (Dzou et al., 1995)

diagenesis through early metagenesis (Radke and Welte, 1983; Dzou et al., 1995). At the same time their values are relatively independent of depositional controls (Marynowski et al., 2000), when compared e.g., to indices based on hopanes and steranes. For our purposes we considered (Table 3) the indices based on methylnaphthalenes (TMN, TeMN), methylphenantrenes (MPI-1, MPR) and methyldibenzothiophenes (MDR), which are commonly applied as indicators of the level of high thermal maturity, showing correlation with vitrinite reflectance values, %Ro (Radke and Welte, 1983; Radke et al., 1986; Dzou et al., 1995). The results (Table 3) show a similar maturation level of the OM for all the samples.

The absence of monoaromatic steroids suggests that all these compounds altered to triaromatics by processes involving aromatization and loss of methyl groups, which indicates that the OM should have a %Ro of over 1.0 (Hunt, 1995). Moreover, when considering the trimethylnaphthalenes in the samples (TMNs, *m/z* 170), the 1,3,7-TMN (αββ) isomer is more abundant than the 1,2,5-TMN (αβα), whereas in the case of the tetramethylnaphthalenes (TeMNs, *m/z* 184), the 1,3,6,7-TeMN (αβββ) isomer is more abundant that the 1,2,5,6 + 1,2,3,5-TeMN (αβαβ + αββα) set (Table 3 and Fig. 9). These are characteristic patterns of OM overmaturation (Alexander et al., 1985; van Aarssen et al., 1999), because the substitutions of the methyl groups in the β-position in the naphthalene structure are more stable with increasing thermal maturity compared to α-substituted isomers (Radke et al., 1994).

Phenantrenes and methylphenantrenes are present in appreciable proportion in all the samples (*m/z* 178 + 192; Fig. 9); from their relative intensities several parameters of thermal maturity are calculated (see Table 3). The values of the methylphenantrene ratio (MPR) are heterogeneously distributed between 1.83 and 5.0; consequently, these do not provide coherent information on the thermal maturity of the OM (Radke and Welte, 1983). In contrast, the methylphenanthrene index, MPI-1 is one of the most widely used maturity parameter based on aromatic hydrocarbons (Radke and Welte, 1983). The parameter relies on a shift with maturity in the methylphenanthrene distribution toward a preponderance of β-type isomers. MPI-1 is often used in estimating the equivalent

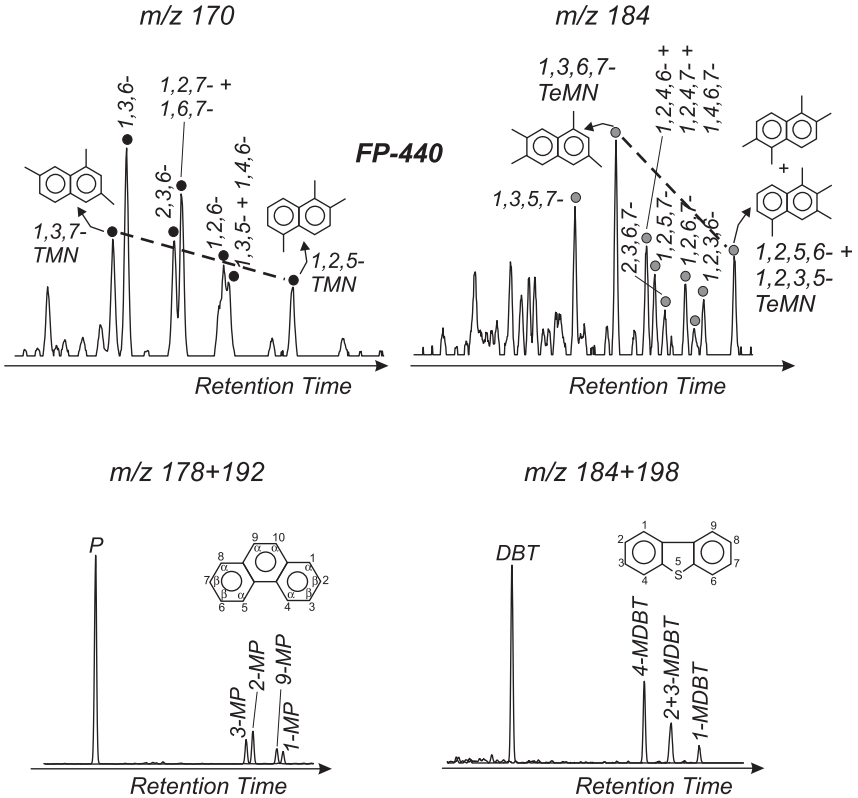

Fig. 9. Distributions of trimethylnaphthalenes (TMNs, *m/z* 170), tetramethylnaphthalenes (TeMNs, *m/z* 184), phenantrene and methylphenantrene (MP) isomers (*m/z* 178 + 192), dibenzothiophene and methyldibenzothiophene (MDBT) isomers (*m/z* 184 + 198) for a characteristic sample from the Pedregoso Formation.

vitrinite reflectance value (%Rc_1) for crude oils and source rock (Radke and Welte, 1983). The MPI-1 and %Rc_1 values calculated for the bitumens of the Pedregoso Formation range from 0.10 to 0.55 (average, 0.40) and 1.97–2.24% (average, 2.11%) respectively (Table 3), another indication that the OM is overmature, specifically, in the dry gas window. The low MPI-1 index values observed in some samples (Table 3) may be due to lithological variations as well as to type of preserved OM (marine origin) (Radke and Welte, 1983; Cassani et al., 1988).

The indices involving aromatic sulfur compounds also can indicate that the OM reaches a high level of thermal maturity at the end of late catagenesis. 1-Methyldibenzothiophene (1-MDBT), 2 + 3-methyldibenzothiphene (2 + 3-MDBT) and 4-methyldibenzothiophene (4-MDBT) are present in appreciable amount in all the samples (m/z 184 + 198; Fig. 9). 4-/1-MDBT ratio (MDR) has been proposed as maturity parameter (Radke et al., 1986; Dzou et al., 1995). The ratio generally increases with increasing maturity and correlates well with vitrinite reflectance of source rock. Thus, the ratio is also useful in calculating equivalent vitrinite reflectance (%Rc_2) value for crude oil and source rock (e.g., Dzou et al., 1995). The MDR and %Rc_2 for the samples range from 3.40 to 13.85 (average, 5.93) and 1.23–1.60% (average, 1.35%) respectively (Table 3). Unexpectedly, the %Rc_2 values suggest that the OM of the Pedregoso Formation is in the oil window, which differs with most of the maturity parameters obtained here.

Rock-Eval T_{max} values can help discern between the different maturity assessments obtained here, i.e., between %Rc_1 and %Rc_2. These measurements range between 478 and 491 °C (average 486 °C; Table 3), indicating that the Pedregoso OM have reached the dry gas window stage, in agreement with the Rc_1 values (Table 3).

5. Discussion

5.1. Sources and preservation of the organic matter

The biomarker distributions strongly suggest that the OM in the Pedregoso Formation is mainly of marine origin. However, the H/C ratios of the kerogen concentrates indicate that the OM is in the type IV domain. Indeed the OM of the Pedregoso Formation was type II -prior to its oxidation and/or thermal alteration- but due to maturation the plot of the present day composition in a Van Krevelen diagram gives type IV. The Pedregoso Formation results mainly from the accumulation of turbidites in a carbonate ramp system, adjacent to the San Luis Reef. The depositional setting must have been submitted to oxic-to-dysoxic conditions. Benthic waters were perhaps not fully oxygenated because of the semi-enclosed configuration of the basin during the Late Oligocene–Early Miocene (Fig. 10). The basin was ventilated by relatively weak currents (Díaz de Gamero, 1977), which probably did not sustain high productivity in surface water. Through the entire formation, TOC values keep close to 1%, either within turbidites or in between. The values are relatively high if one considers that marine OM is labile and that the depositional redox conditions were not very favorable to OM preservation. It suggests that the marine OM, either settling from the photic zone or reworked from shallower parts of the ramp and embedded within turbidites, was partly protected from oxidation by rapid burial, thanks to the accumulation of turbidites, preventing protracted residence of OM in oxygen-containing bottom waters. Of course, this partial protection could not prevent the activity of anaerobic bacteria within the sediments.

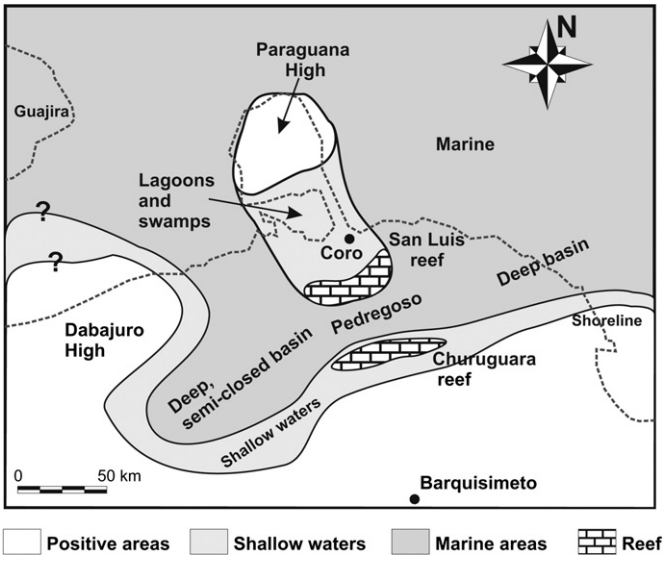

Fig. 10. Paleogeographic reconstruction of the Falcón Basin during Pedregoso sedimentation (modified from Díaz de Gamero, 1977).

5.2. Thermal maturity of organic matter and burial depth of the Pedregoso Formation

The Falcón Basin is included in a complex geological setting influenced by tectonic processes driven by the junction between the Caribbean, Nazca and South America plates (Audemard, 2001; Bezada et al., 2007; among others). Likewise, outcrops of intrusive igneous bodies occur along the axis of the Falcón Basin and have been associated with crustal thinning during Late Eocene–Early Miocene times (Sousa et al., 2005; Bezada et al., 2007). This tectonic event was accompanied by an abnormal increment of the heat flow (~190 mW m^{-2}) of the region that significantly affected the maturation of the source rocks in the Falcón Basin (Baquero et al., 2009). Hence, the sedimentary burial and anomalous increase in the geothermal gradient in the region could have been the factors responsible for OM maturation.

The OM in the Pedregoso Formation is overmature, in relation with a deep burial by post-Oligocene deposits. North to the Falcón Basin, the Pedregoso Formation is reported to have been buried below more than 3050 m of sediments in the La Vela Bay (Fig. 1b; Boesi and Goddard, 1991). In the central part of the Falcón Basin, the maximum possible burial is estimated to reach 6.5 km (Table 4). This thickness is obtained by summing the thicknesses of the respective formations overlying the Pedregoso Formation (e.g., Díaz de Gamero, 1977; González de Juana et al., 1980; PDVSA, 2009).

Table 4
Stratigraphic thickness values reported in the literature (Díaz de Gamero, 1977; González de Juana et al., 1980; PDVSA, 2009) for the formations in the central part of the Falcón Basin (Urumaco Trough). The values for the Pedregoso Formation are emphasized in bold.

Urumaco Trough		
Formation	Stratigraphic thickness (km)	Accumulated stratigraphic thickness (km)
Urumaco	1.67	1.67
Socorro	1.57	3.24
Querales	0.57	3.81
Cerro Pelado	1.00	4.81
Agua Clara	1.7	**6.51**[a]
Pedregoso	0.68	7.19
Pecaya	2.00	9.19
Paraíso	1.00	

[a] Depth of burial (measured in field) for the Pedregoso Fm. used in Fig. 11.

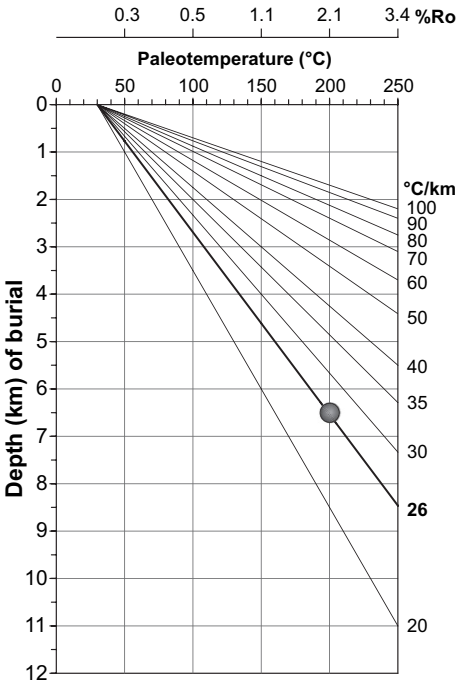

Fig. 11. Estimated range of paleotemperature and equivalent paleodepth for the Early Miocene Pedregoso Formation. We assumed a geothermal gradient of 26 °C/km and a surface temperature of 30 °C for the central region of the Falcón Basin according to Baquero et al. (2009).

The maximum depth of burial of the Pedregoso Formation also can be estimated (Fig. 11) using maturity parameters derived from the aromatic-biomarker distribution (2.1%Rc_1) and T_{max} values (~486 °C) from Rock-Eval pyrolysis (Table 3) and geothermal data for the central region of the Falcón Basin determined by Baquero et al. (2009). A maximum paleotemperature of 200 °C can be calculated using the relation:

$$\%Ro = 7.785 \cdot 10^{-5} \cdot T^2 - 7.610 \cdot 10^{-3} \cdot T + 0.4633$$

In this formula – derived from two-dimensional thermal calibration from the Falcón Basin (see discussion in Baquero et al., 2009) – T (°C) and %Ro are the maximum paleotemperature and the vitrinite reflectance (~2.1) respectively. Assuming a geothermal gradient of 26 °C/km and a surface temperature of 30 °C (Baquero et al., 2009), and considering a maximum paleotemperature of 200 °C, the estimated depth of burial is 6.5 km (Fig. 11). This value is in accordance with that obtained from stratigraphic thicknesses in the Urumaco Trough (Table 4). This implies that: (1) the geothermal gradient was normal during and after the deposition of the Pedregoso Formation, (2) the OM maturation in this unit is due to the sedimentary burial. Therefore, if an increase of the geothermal gradient occurred in the Falcón Basin (Sousa et al., 2005; Bezada et al., 2007), this increase occurred before the Pedregoso Formation was deposited, and/or the thermal anomaly did not reach the study area. Similar results are reported in relation to the Pecaya Formation in the central part of the Falcón Basin (Baquero et al., 2009). Finally, the vitrinite reflectance vs. burial depth diagram (Fig. 11) could be used as an indirect method for determination of the maximum burial depth and paleotemperature reached by different formations in the area.

To conclude, the Pedregoso type-II OM (marine origin) and initial organic richness value (TOC ~1.8%) suggest that this unit has probably generated hydrocarbons within the Urumaco Trough, in agreement with Boesi and Goddard (1991), who indicated that the Pedregoso Formation was an oil source rock north to the Falcón Basin. However, a high present-day thermal maturity (dry gas window) of the Pedregoso Formation indicates that this unit is only capable to generate gas. These interpretations are in accordance with the thermal modelling of the Falcón Basin (Baquero et al., 2009), which suggests that hydrocarbon accumulations are mainly located on the northern flanks, with small amounts possible in the central part of the basin (e.g., the Urumaco Trough).

6. Summary and conclusions

The results of this research provide the following generalizations and conclusions:

1. The inorganic (TOC–S–Fe, DOP) and organic (Pr/Ph) geochemical parameters suggest that the predominating paleooxygenation conditions during the deposition of the sediments of the Pedregoso Formation (Early Miocene) were oxic-to-dysoxic.
2. The distributions of saturated biomarkers indicate the organic matter is mainly of marine origin, deposited in a marine carbonate environment. Organic productivity was likely high, consistent with the presence of reefal systems.
3. The low variability seen in the TOC concentrations of the carbonate-free fraction, as well as in the distributions of saturated and aromatic biomarkers, suggest that the environmental conditions and the supply of organic matter remained relatively constant throughout the sedimentation of the Pedregoso Formation.
4. The Pedregoso Formation is a "spent" oil source rock within the Urumaco Trough, in the Falcón Basin. This interval initially had good hydrocarbon potential (high TOC, Type-II OM), but is now in the overmature stage of hydrocarbon generation (dry gas window).
5. The maturity reached by the organic matter contained in the Pedregoso Formation is consistent with the depth that this unit was buried. This suggests that the thermal anomaly that affected the basin did not reach the central part of the basin or did not reach the Early Miocene, and therefore, the organic matter maturation in this unit is due to the sedimentary burial.

Acknowledgments

This research was funded by the "Consejo de Desarrollo Científico y Humanístico de la UCV", through the projects 03.00.5751.2004 and 03.00.5857.2005, and it is a contribution of the Laboratoire Géosystèmes, UMR 8157 CNRS (Université Lille 1). We also thank Christine Laurin for technical assistance. The authors are grateful to François Baudin (Université Pierre et Marie Curie – Paris 6) for performing the Rock-Eval analyses. Marvin Baquero (PDVSA-Exploration) is thanked for constructive discussions, which helped to improve the original version of this work. Thanks to the two reviewers (Jean-Robert Disnar and Frederic Schneider) for improving this manuscript through careful review, and to Hanneke Verweij for his editorial work.

References

Alberdi, M., López, L., 2000. Biomarker 18α(H)-Oleanane: a geochemical tool assess Venezuelan petroleum systems. Journal of South American Earth Science 13, 751–760.

Alexander, R., Kagi, R.I., Roland, S.J., Sheppard, P.N., Chirila, T.V., 1985. The effects of thermal maturity on distributions of dimethylnaphthalenes and trimethylnaphthalenes in some ancient sediments and petroleums. Geochimica et Cosmochimica Acta 49, 385–395.

Alexander, R., Strachan, M.G., Kagi, R.I., Van Bronswijk, W., 1986. Heating rate effects on aromatic maturity indicators. Organic Geochemistry 10, 997–1003.

Audemard, F.A., 2001. Quaternary tectonics and present stress tensor of the inverted northern Falcón Basin, northwestern Venezuela. Journal of Structural Geology 23, 431–453.
Baquero, M., Acosta, J., Kassabji, E., Zamora, J., Sousa, J.C., Rodriguez, J., Grobas, J., Melo, L., Schneider, F., 2009. Polyphase development of the Falcon Basin in northwestern Venezuela: implications for oil generation. In: James, K.H., Lorente, M.A., Pindell, J.L. (Eds.), The Origin and Evolution of the Caribbean Plate. Geological Society, London, Special Publications, vol. 328, pp. 585–610.
Berner, R.A., 1984. Sedimentary pyrite formation: an update. Geochimica et Cosmochimica Acta 48, 605–615.
Bezada, M., Schmitz, M., Jácome, M.I., Rodríguez, J., Audemard, F., Izarra, C., 2007. Crustal structure in the Falcón basin area, northwestern Venezuela, from Seismic and Gravimetric evidence. Journal of Geodynamics 45, 191–200.
Blumer, M., Guillard, R.R.L., Chase, T., 1971. Hydrocarbons of marine phytoplankton. Marine Biology 8, 183–189.
Boesi, T., Goddard, D., 1991. A new geology model related to the distribution of hidrocarbon source rocks in the Falcón Basin, Northwestern Venezuela. American Association of Petroleum Geology Memoirs 52, 303–319.
Bray, E.E., Evans, E.D., 1961. Distribution of n-paraffins as a clue to recognition of source beds. Geochimica et Cosmochimica Acta 22, 2–15.
Cassani, F., Gallando, O., Talukdar, S., Vallejos, C., Ehrmann, U., 1988. Methylphenanthrene maturity index of marine source rock extracts and crude oils from the Maracaibo Basin. Advances in Organic Geochemistry 13, 73–80.
Dean, W.E., Arthur, M.A., 1989. Iron-sulfur-carbon relationships in organic-carbon-rich sequences: cretaceous Western Interior Seaway. Science 289, 708–743.
Del Ollo, D., Escandón, D.M., Galarraga, F., 1994. Origin of petroleum in the Falcón basin. Memorias del V Simposio de Exploración Petrolera en las Cuencas Subandinas, 408–410.
Díaz de Gamero, M.L., 1977. Stratigraphy and micropaleontology of the Oligocene and early Miocene for the center of the Falcón basin, Venezuela. Geos 22, 3–60.
Díaz de Gamero, M.L., 1989. Early and middle Miocene for the north Falcón. Geos 29, 25–35.
Dzou, L.I., Noble, R.A., Sentfle, J.T., 1995. Maturation effects on absolute biomarker concentration in a suite of coals and associated vitrinite concentrates. Organic Geochemistry 23, 681–697.
Ekweozor, C.M., Udo, O.T., 1987. The oleananes: origin, maturation and limits of occurrence in southern Nigeria sedimentary basin. In: Matavelli, L., Novelli, L. (Eds.), Advances in Organic Geochemistry, vol. 13, pp. 131–141.
Espitalié, J., Deroo, G., Marquis, F., 1986. La pyrolyse Rock Eval et ses applications. Revue de l'Institut Français du Pétrole 40 (B), 755–784.
Gelpi, E., Schneider, H., Mann, J., Oro, J., 1970. Hydrocarbons of geochemical significance in microscopic algae. Phytochemistry 9, 603–612.
Ghosh, S., Pestman, P., Meléndez, L., Truskowski, I., Zambrano, E., 1997. Tectonostratigraphic evolution and petroliferous systems of the Falcón Basin, northwestern Venezuela. Memoirs of the VIII Venezuelan Geological Congress I, 317–329.
González de Juana, C., Arozena, J., Picard, C., 1980. Geology of Venezuela and Its Petroliferous Basins, vol. I and II. Fonvises Editions, Caracas, p. 1031.
Hesse, P.R., 1971. A Textbook of Soil Chemical Analysis. John Murray Publishers, London.
Hetényi, M., Sajgó, C., Vetö, I., Brukner-Wein, A., Szántó, Z., 2004. Organic matter in a low productivity anoxic intraplatform basin in the Triassic Tethys. Organic Geochemistry 35, 1201–1219.
Huang, W.Y., Meinschein, W.G., 1979. Sterols as ecological indicators. Geochimica et Cosmochimica Acta 43, 739–745.
Huerta-Díaz, M.A., Morse, J.W., 1990. A quantitative method for determination of trace metal concentrations in sedimentary pyrite. Marine Chemistry 29, 119–144.
Hughes, W.B., Holba, A.G., Dzou, L.I.P., 1995. The ratios of dibenzothiophene to phenanthrene and pristane to phytane as indicators of depositional environment and lithology of petroleum source rocks. Geochimica et Cosmochimica Acta 59, 3581–3598.
Hunt, J., 1995. Petroleum Geochemistry and Geology, second ed. Freeman and company, San Francisco, p. 385.
Koopmans, M.P., Rijptra, W.I., Klapwijk, M.M., de Leew, J.W., Lewan, M.D., Sinninghe Damsté, J.S., 1999. A thermal and chemical degradation approach to decipher pristane and phytane precursors in sedimentary organic matter. Organic Geochemistry 30, 1089–1104.
Macellari, C., 1995. Cenozoic sedimentation and tectonics of the southwestern Caribbean pull-apart basin, Venezuela and Colombia. American Association of Petroleum Geology Bulletin 62, 757–780.
Marynowski, L., Narkiewicz, M., Grelowski, C., 2000. Biomarkers as environmental indicators in a carbonate complex, examples from the middle Devonian, the Holy Cross Mountains, Poland. Sedimentary Geolology 137, 187–212.
Noya, J., 2001. Study of the Origin and Sedimentation Environment of the Pedregoso Formation, Falcón State. Universidad Central de Venezuela, Escuela de Química, BSc thesis, 87 p.
Nytoft, H.P., Bojesen-Koefoed, J.A., Christiansen, F.G., Fowler, M.G., 2002. Oleanane or lupane?: reappraisal of the presence of oleanane in Creataceous-Tertiary oils and sediments. Organic Geochemistry 33, 1225–1240.
Ostos, M., Yoris, F., Avé Lallemant, H., 2005. Overview of the southeast Caribbean-South American plate boundary zone. In: Avé Lallemant, H.G., Sisson, V.B. (Eds.), Caribbean–South American Plate Interactions, Venezuela. Geological Society, America, Special Paper, vol. 394, pp. 53–90.
Ourisson, G., Albrecth, P., Rohmer, M., 1982. Predictive microbial biochemistry from molecular fossils to procaryotic membranes. Trends in Biochemical Sciences 7, 236–239.
Ourisson, G., Albrecht, P., 1992. Hopanoids. 1. Geohopanoids: the most abundant natural products on Earth? Accounts of Chemical Research 25, 398–402.
Ourisson, G., Rohmer, M., 1992. Hopanoids. 2. Biohopanoids: a novel class of bacterial lipids. Accounts of Chemical Research 25, 403–408.
PDVSA, 2009. Stratigraphic code of the Venezuelan petroliferous basins. Online at: Petroleum de Venezuela www.pdvsa.com/lexico/lexicoh.htm (revised in May 2009).
Peters, K., Walters, C., Moldowan, J., 2005. The Biomarker Guide. Biomarkers and Isotopes in Petroleum Systems and Earth History, second ed. Cambridge University Press, Cambridge, 1132 p.
Radke, M., Welte, D.H., 1983. The methylphenantrene index (MPI): a maturity parameter based on aromatic hydrocarbons. In: Bjoroy, M., Albrecht, C., Cornford, C., de Groot, K., Eglinton, G., Galimov, E., Leythaeuser, D., Pelet, R., Rullkoetter, J., Speers, G. (Eds.), Advances in Organic Geochemistry. J. Wiley and sons, New York, pp. 504–512.
Radke, M., Welte, D.H., Willsch, H., 1986. Maturity parameters based on aromatic hydrocarbons: influence of the organic matter type. Organic Geochemistry 10, 51–63.
Radke, M., Rullkotter, J., Vriend, S.P., 1994. Distribution of naphthalenes in crude oils from the Java Sea: source and maturation effects. Geochimica et Cosmochimica Acta 58, 3675–3689.
Raiswell, R., Buckley, F., Berner, R.A., Anderson, T.F., 1987. Degree of pyritization of iron as a palaeoenvironmental indicator of bottom-water oxygenation. Journal of Sedimentary Petrology 58, 812–819.
Rimmer, S.M., Thompson, J.A., Goodnight, S.A., Robl, T.L., 2004. Multiple controls of the preservation of organic matter in Devonian-Mississippian marine black shales: geochemical and petrographic evidence. Palaeogeography, Palaeoclimatology, Palaeoecology 215, 125–154.
Rojas, H., 2001. Chemostratigraphy of the Pedregoso Formation, Falcón State: Redox Variations and Cyclical Patterns. Universidad Central de Venezuela, Escuela de Química, BSc thesis, 96 p.
Sousa, J., Rodríguez, J., Giraldo, C., Rodríguez, I., Audemard, F.A., Alezones, R., 2005. An integrated geological–geophysical profile across northwestern Venezuela. In: Presented at the Sixth International Symposium on Andean Geodynamics Barcelona, Spain.
Tissot, B., Demaison, G., Masson, P., Delteil, J.R., Combaz, A., 1980. Paleoenvironment and petroleum potential of middle Cretaceous black shales in Atlantic basins. American Association of Petroleum Geologists Bulletin 64, 2051–2063.
Tissot, B.P., Welte, D.H., 1984. Petroleum Formation and Occurrence. Springer-Velarg, 699 p.
van Aarssen, B.G., Bastow, T.P., Alexander, R., Kagi, R.I., 1999. Distributions of methylated naphthalenes in crude oils: indicators of maturity, biodegradation and mixing. Organic Geochemistry 30, 1213–1227.
Vandenbroucke, M., Largeau, C., 2007. Kerogen origin, evolution and structure. Organic Geochemistry 38, 719–833.
Volkman, J.K., Barrett, S.M., Blackburn, S.I., Mansour, M.P., Sikes, E.L., Gelin, F., 1998. Microalgal biomarkers: a review of recent research developments. Organic Geochemistry 29, 1163–1179.